

STUDY OF THE BEAM-BEAM INTERACTION IN AN ELECTRON-POSITRON COLLIDER WITH LARGE PIWINSKI ANGLE AND CRABBED WAIST*

S. Li, C. Zhang, T. Liu, Q. Luo[†], University of Science and Technology of China, Hefei, China

Abstract

To achieve very high luminosity, the next generation circular colliders adopt the crab waist collision scheme with a large Piwinski angle. In this scheme, beams collide with high current, low emittances, and small beta functions at the interaction point (IP). However, several effects arising from these extreme parameters, especially the coherent X-Z instability, will significantly impact the collider's performance, necessitating dynamic processing of longitudinal motion in a three-dimensional self-consistent treatment. The transverse vibration becomes coupled with the longitudinal motion, as well as the increase in horizontal beam size alters the interaction between beams and corresponding beam-induced effects. These instabilities limit the stable high luminosity area for the selected working point of the original design. Therefore, it is necessary to optimize the safe area of the working point by readjusting the parameters of the IP. In this paper, based on the preliminary conceptual design Super Tau-Charm Facility (STCF) project in China, the instabilities caused by beam interactions is studied through numerical simulation. The relationship between the parameters at the IP and the stable selection area of the working point is systematically explored. The regularities found from simulations can assist future high luminosity electron-positron colliders in selecting the corresponding parameters. Additionally, some methods, such as adding adjustable devices to achieve stable high luminosity, are also proposed.

INTRODUCTION

Super Tau-Charm Facility (STCF) is an electron-positron collider proposed by the Chinese particle physics community [1]. The STCF is designed to operate in a center-of-mass energy range from 2 to 7 GeV with a peak luminosity of $0.5 \times 10^{35} \text{ cm}^{-2} \text{ s}^{-1}$ or higher.

STCF with its high luminosity can generate more physical events, reducing statistical error and making rare events observable. It's designed as a double ring electron-positron collider with a 2 A beam current and a longitudinally polarized electron beam. The beams circulate in separate rings and intersect at a single Interaction Point (IP) where a detector is placed. The rings have the same lattice structure, including the straight section, but the electron storage ring will have five Siberian Snakes on its straight section for longitudinal polarization at the IP in the future [2]. The

* Work supported by the National Key R&D Program of China under Contract No. 2022YFA1602201, the National Natural Science Foundation of China No.12105278, the Quality Engineering Project for Anhui Province Higher Education Institutions No.2021jyxm1731 and the International Partnership Program of the Chinese Academy of Sciences Grant No. 211134KYSB20200057.

† luoqing@ustc.edu.cn

design parameters of the initial version are shown in Table 1.

The STCF will use a new collision scheme based on large Piwinski angle and crab waist sextupoles to increase luminosity. Strong-strong simulations can reveal a novel coherent beam-beam instability related with v_s and v_x based on large-crossing-angle-crab-waist collision [3]. The IBB code for beam-beam simulation developed by Yuan Zhang adopts PIC architecture and can simulate the large cross angle collision on crab waist schema [4], and further studies on X-Z instability have been validated by this code [5]. This article used IBB to simulate the beam-beam interaction of STCF.

SIMULATION RESULTS ANALYSIS

The simulation results in this part are based on the initial lattice parameters in Table 1.

Pre-scan for Luminosity

Firstly, we determine the general selection range of v_y to be around 0.570 by scanning it on fixed $v_x = 0.540$ which is the design working point. We changed v_x in a small range and changed v_y in a large range for two alternative ranges of v_x . The result after tracking one-damping-time turns is shown in Fig. 1, the horizontal and vertical coordinates are the fractional parts of the tune. The left one has more areas of luminosity greater than $9.75 \times 10^{34} \text{ cm}^{-2} \text{ s}^{-1}$ where v_x is in $0.550 \sim 0.555$, but the right one where v_x is in $0.568 \sim 0.571$ has more areas of luminosity greater than $9.60 \times 10^{34} \text{ cm}^{-2} \text{ s}^{-1}$. For different v_x , v_y of high luminosity area is very close, so we can fix $v_y = 0.570$, horizontal scan v_x in strong-strong simulation.

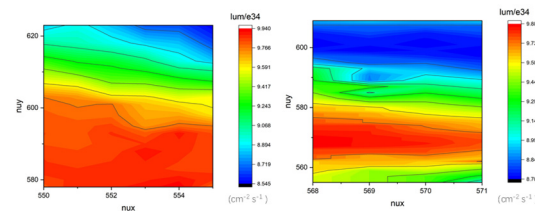


Figure 1: Luminosity with the scan of v_x and v_y of two ranges.

Beam Size Tracking

At the same time, we find that luminosity drops extremely at some v_x . Due to the nonlinearity of beam interaction, strong diffusion along the high-order transverse resonance results in a serious increase in the transverse beam size. By tracking the beam size, we can see that the horizontal beam size increases more than the vertical beam size

at the working points where luminosity drops sharply (Fig. 2).

Table 1: Parameters of Lattice

Parameters	Original Version	Adjusted Version
Circumference / m	707.258	702
Beam Energy / GeV	2*, 1-3.5	2*, 1-3.5
Crossing Angle (θ_0) / mrad	60	60
Current / A	1.5	2
Damping time (x/y/z)/ms	54/54/27	32/32/16
$(\beta_x^*/\beta_y^*)/\text{mm}$	64.1/0.638	90/0.6
$(\varepsilon_x/\varepsilon_y)/\text{nm}\cdot\text{rad}$	2.85/0.0285	4.167/0.0208
$v_x/v_y/v_s$	30.523/28.53 8/0.016	30.537/28.57 0/0.016
Momentum Compaction Factor	1.237×10^{-3}	7.20×10^{-4}
Energy Spread	4.034×10^{-4}	7.19×10^{-4}
$(\sigma_x/\sigma_y)/\mu\text{m}$	13.61/1.39	19.37/0.1117
ξ_x	0.005	0.00389
ξ_y	0.04-0.06 (estimate)	0.008549
Hour-glass Factor	0.8 (estimate)	0.9
Luminosity / $10^{35}\text{cm}^{-2}\text{s}^{-1}$	0.63-0.95	1.1

Problems existed at that time: $\xi_x \sim 0.005$ was too large, and the x direction blew up badly. In the next section, we will add some adjustable devices to the design lattice to change the beam parameters to obtain a more stable luminosity range.

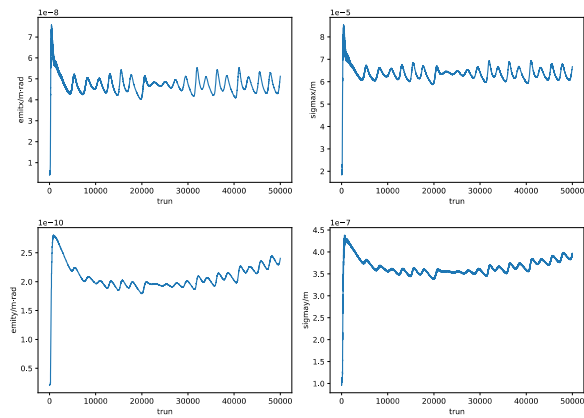


Figure 2: A comparison of bunch size tracking between X and Y direction.

X-Z Instability

Recent studies have shown that beam-beam interactions at large Piwinski angle give rise to a new type of coherent head-tail instability. Due to the beam force, the transverse vibration will be affected by the longitudinal dynamics, and the increase of the horizontal beam size will change the interaction between the beams and the corresponding beam-induced effects [5]. This instability, known as X-Z instability, cannot be suppressed through beam feedback systems but can only be avoided through appropriate parameter optimization, generates resonance lines with peak intervals that are exactly multiples of v_s . Fig. 3 shows the emittance growth rate with v_x of $v_s = 0.016$, the emittance increases dramatically at the peak of the X-Z instability resonance line where the luminosity decreases dramatically.

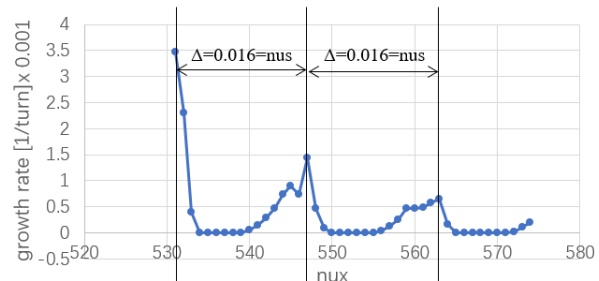


Figure 3: Emittance growth rate with v_x .

Typically, to prevent luminosity from being affected, a stringent requirement of $\xi_x \ll v_s$ is imposed. In the case of STCF, v_s is at least 3 times larger than ξ_x [6].

MITIGATION METHOD

We changed the beam parameters to obtain a more stable luminosity region by adding some adjustable devices to the design lattice. The optimized parameters are shown in Table 1.

Higher Order Harmonic Cavity

In order to increase luminosity and prevent beam loss due to X-directional blow-up, we aim to incorporate a

higher harmonic cavity. This addition will allow us to adjust sigma z as a variable, facilitating synchronous changes in various parameters amidst complex coupling constraints. Based on the original lattice, the beam length is adjusted from 12.2 mm to 10 mm, and the luminosity of the first circle is increased to $1.34e35$ by increasing ξ_y by 1.22 times. Reduce the β_x to 9 cm to obtain $\xi_x < 0.004$, avoiding transverse bunch size explosion. Make the size of the X-direction bunch decreases simultaneously with constant emittance. And in order to suppress the hourglass effect, the β_y must also be reduced simultaneously which equal to 0.6 mm close to $\sigma_x / 2\theta$ (0.644 mm).

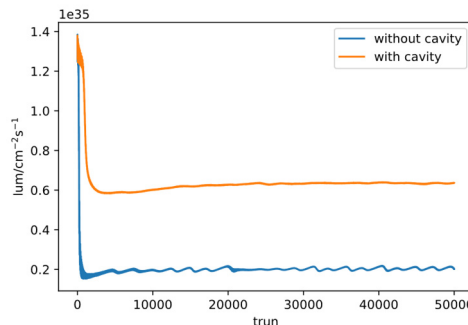


Figure 4: Luminosity with and without higher order harmonic cavity.

The improved luminosity effect is shown in Fig. 4. We also need to keep $v_s \sim 3 \xi_x$ after reducing β_x and β_y to make the safe gap of the resonance lines which is from the X-Z instability wider.

Damping Wigglers

At the same time, in order to further improve the luminosity, damping wigglers are adopted to obtain a faster stable beam to obtain a higher luminosity and achieve the damping time target of 36 ms (Fig. 5). The reserved length of the linear section is 4×2 m. Four damping wigglers of 1.8m are set (Table 2).

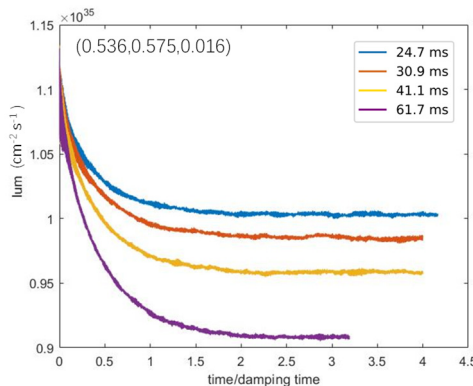


Figure 5: Luminosity at different damping times.

Table 2: Design Parameters of DW

Parameter	Value	Unit
Single DW length	1.8	m
Period	20	cm
Number of DW	4	
Field quality ($x=1$ cm)	$<10^{-3}$	

In order to reach the required damping time of 32 ms, taking the design working energy as an example, the parameters required for each damping wiggler to meet the field strength are shown in Table 3. When the operating energy reaches 2.5 GeV, the radiation damping is sufficient without the need for DW to control the damping time.

Table 3: Parameters of Per DW

Energy (GeV)	Wiggler field B_w (T)	Wiggler SR power (kW)	Damping integral (T ² m)
1	5.1	59.3	23.41
1.5	3.7	70.2	12.32
2	2.3	48.2	4.76
2.5	0	0	0

SUMMARY AND OUTLOOK

In this paper, a self-consistent beam-beam simulation code is used to verify the luminosity of the lattice parameters of STCF design. Through the scanning of the working points, the high-luminosity working point area is obtained and the X-Z instability caused by the crab waist scheme is observed. In order to achieve the design target and obtain a more stable working point area as much as possible, we designed to add adjustable devices such as higher harmonic cavities and damping wiggler to optimize the lattice parameters, which will reach the design target of more than $1 \times 10^{35} \text{ cm}^{-2}\text{s}^{-1}$. However, there is still space for further optimization, and the instability caused by impedance and lattice nonlinearity has not been considered at present, so further optimization parameters and simulation research are needed.

ACKNOWLEDGEMENTS

The first author would like to thank Y. Zhang (IHEP), K. Ohmi (KEK) and D. Zhou (KEK) for their guidance helps. We thank the Hefei Comprehensive National Science Center for their strong support on the STCF key technology research project.

REFERENCES

[1] H.P. Peng, Y.H. Zheng and X.R. Zhou, "Super Tau-Charm Facility of China", *Physics*, vol. 49, no. 8, pp. 513–524, Aug. 2020. doi: [10.7693/w120200803](https://doi.org/10.7693/w120200803)

[2] J. Q. Lan *et al.*, "Design of beam optics for a Super Tau-Charm Factory," *J. Inst.*, vol. 16, no. 07, p. T07001, Jul. 2021. doi: [10.1088/1748-0221/16/07/T07001](https://doi.org/10.1088/1748-0221/16/07/T07001)

[3] K. Ohmi *et al.*, "Coherent Beam-Beam Instability in Collisions with a Large Crossing Angle," *Phys. Rev. Lett.*, vol. 119, no. 13, p. 134801, Sep. 2017. doi: [10.1103/PhysRevLett.119.134801](https://doi.org/10.1103/PhysRevLett.119.134801)

[4] Y. Zhang, K. Ohmi, and L. Chen, "Simulation study of beam-beam effects," *Phys. Rev. ST Accel. Beams*, vol. 8, no. 7, p. 074402, Jul. 2005. doi: [10.1103/PhysRevSTAB.8.074402](https://doi.org/10.1103/PhysRevSTAB.8.074402)

[5] Y. Zhang *et al.*, "Self-consistent simulations of beam-beam interaction in future e + e – circular colliders including beam-strahlung and longitudinal coupling impedance," *Phys. Rev. Acc. Beams*, vol. 23, Oct. 2020. doi: [10.1103/PhysRevAccelBeams.23.104402](https://doi.org/10.1103/PhysRevAccelBeams.23.104402).

[6] L. Zhang *et al.*, "Longitudinal beam dynamics design for Super Tau-Charm Facility", in *Proc. 14th Symposium on Accelerator Physics (SAP'2023)*, Xichang, China, *arXiv*, Mar. 2024. doi: [10.48550/arXiv.2403.00308](https://doi.org/10.48550/arXiv.2403.00308).